International Journal of Mechanical, Industrial and Aerospace Sciences
ISSN: 2517-9950
Vol:6, No:4, 2012

Effect of Swirl on Gas-Fired Combustion Behavior in a 3-D Rectangular Combustion Chamber

Man Young Kim

Abstract**—**The objective of this work is to investigate the turbulent reacting flow in a three dimensional combustor with emphasis on the effect of inlet swirl flow through a numerical simulation. Flow field is analyzed using the SIMPLE method which is known as stable as well as accurate in the combustion modeling, and the finite volume method is adopted in solving the radiative transfer equation. In this work, the thermal and flow characteristics in a three dimensional combustor by changing parameters such as equivalence ratio and inlet swirl angle have investigated. As the equivalence ratio increases, which means that more fuel is supplied due to a larger inlet fuel velocity, the flame temperature increases and the location of maximum temperature has moved towards downstream. In the mean while, the existence of inlet swirl velocity makes the fuel and combustion air more completely mixed and burnt in short distance. Therefore, the locations of the maximum reaction rate and temperature were shifted to forward direction compared with the case of no swirl.

Keywords**—**Gaseous Fuel, Inlet Swirl, Thermal Radiation, Turbulent Combustion

I. Introduction

DURING the past few decades, the calculation of turbulent combusting flows has received considerable attention to meet the future regulation of NOx and N_2O emission. As a consequence of the growth in the related literature, considerable progress has been made in understanding the various calculation procedures and the NOx formation and removal. Emissions from conventional combustor such as boiler, gas turbine, and pulverized coal combustors, however, requires a more fundamental analyses and has led to an increased demand for numerical predictions in turbulent reacting flow [1]. Despite the continued developments of empirical and theoretical analyses for combustion technology in various combustion cambers, the challenge which a engineer faces today to ingenuity in combustor design is greater than ever before due mainly to the environmental regulations as well as energy conservation and higher efficiency [2].

If is widely known that oxides of nitrogen (NOx), which is formed via chemical reactions between oxygen in air and nitrogen in fuel as well as in air, account for acid rain, photochemical smog, and about 50% of the stratospheric ozone depletion, and exerting direct impacts on health. Nitric oxide formation in turbulent flame, however, is complex because of its strong dependence on such various factors as aerodynamic strain [3], radiative cooling, superequilibrium oxygen chemistry [4] and prompt NO chemistry [5]. Therefore, a typical CFD code adopts a fast-chemistry combustion model to predict turbulent gaseous flames and the Zeldovich kinetic mechanism, with some equilibrium hypothesis, to model thermal NO formation. Despite to these simplifying assumptions, reasonable results for global NO emissions have been reported, in many different situations where flow field mainly influences combustion, with suitable consideration of the interaction between turbulence and pollutant kinetics.

The objective of this work is to find the effect of inlet swirl in a three-dimensional gas-fired combustion chamber by using the numerical methods with finite-volume radiation. That will be a cornerstone work for future application to modeling of combustion-generated pollutant such as NO in a practical engineering combustor. The following sections describe the methodology and models adopted and present various results. Finally, some concluding remarks are addressed to complete this work.

Man Young Kim, Associate Professor, Chonbuk National University, Jeonju, Jeonbuk 561-756, Korea (e-mail: manykim@jbnu.ac.kr).

II. Mathematical Models

A. The Mean Flow Equations

For gas-fueled flames, the local values of velocity, enthalpy and concentration of chemical species can be represented by the following expressions :

Continuity

$$\frac{\partial}{\partial x_j}\left(\rho u_j\right)=0 \tag{1}$$

Momentum

$$\frac{\partial}{\partial x_j}\left(\rho u_i u_j\right)=-\frac{\partial p}{\partial x_i}+\frac{\partial}{\partial x_j}\left[\mu_{eff}\left(\frac{\partial u_i}{\partial x_j}+\frac{\partial u_j}{\partial x_i}\right)\right] \tag{2}$$

where μ_{eff} contains both molecular and turbulent eddy viscosities, i.e., $\mu_{eff}=\mu+\mu_T$.

Energy

$$\frac{\partial}{\partial x_j}\left(\rho u_j h\right)=\frac{\partial}{\partial x_j}\left(\frac{\mu_{eff}}{\mathrm{Pr}_T}\frac{\partial h}{\partial x_j}\right)+H_v\dot{\omega}_{fu}-\nabla\cdot q^R \tag{3}$$

where Pr_T is Prandtl number and h represents the specific enthalpy defined as

$$h=\sum_k Y_k h_k=\sum_k Y_k\int_{T_{ref}}^{T} C_{p,k}(T)\,dT \tag{4}$$

Note that Eq. (3) contains two different source terms due to chemical reaction and radiation. Here, $H_v\dot{\omega}_{fu}$ is the source term due to combustion, while $-\nabla\cdot q^R$ represents the radiation source term.

Chemical Species

$$\frac{\partial}{\partial x_j}\left(\rho u_j Y_i\right)=\frac{\partial}{\partial x_j}\left(\frac{\mu_{eff}}{\mathrm{Sc}_T}\frac{\partial Y_i}{\partial x_j}\right)+\dot{\omega}_i \tag{5}$$

where Y_i and $\dot{\omega}_i$ denote the mass fraction and rate of production of species i, respectively. For simplicity, Pr_T and Sc_T are taken to be 0.9 here.

B. The Turbulence Model

The approach to the turbulence models commonly used for turbulent reacting flows is a form of the two-equation model introduced by Launder and Spalding [6]. The model involves two turbulent transport properties, turbulent kinetic energy k and its dissipation rate ε, where the values of which are obtained from the following transport equations :

Turbulent Kinetic Energy

$$\frac{\partial}{\partial x_j}\left(\rho u_j k\right)=\frac{\partial}{\partial x_j}\left(\frac{\mu_{eff}}{\sigma_k}\frac{\partial k}{\partial x_j}\right)+G_k-\rho\varepsilon \tag{6}$$

Dissipation Rate of the Turbulent Kinetic Energy

$$\frac{\partial}{\partial x_j}\left(\rho u_j \varepsilon\right)=\frac{\partial}{\partial x_j}\left(\frac{\mu_{eff}}{\sigma_\varepsilon}\frac{\partial \varepsilon}{\partial x_j}\right)+C_1\frac{\varepsilon}{k}G_k-C_2\rho\frac{\varepsilon^2}{k} \tag{7}$$

where G_k represents the rate of production of turbulent kinetic energy defined as

$$G_k=\mu_T\left(\frac{\partial u_i}{\partial x_j}+\frac{\partial u_j}{\partial x_i}\right)\frac{\partial u_i}{\partial x_j} \tag{8}$$

The turbulent (or eddy) viscosity is determined by

$$\mu_T=C_\mu\rho k^2/\varepsilon \tag{9}$$

The assumptions involved in these equations have been extensively discussed by Launder and Spalding [6]. Values of empirical constants used in these transport equations are assigned the following values :

$$C_1=1.44, C_2=1.92, C_\mu=0.09, \sigma_k=1.3, \sigma_\varepsilon=1.0 \tag{10}$$

C. The Global Combustion Chemistry

In this work, as a specific example, combustion of methane with air in the idealized irreversible one step is considered as :

$$\mathrm{CH_4}+\nu_{\mathrm{O2}}\left(\mathrm{O_2}+n\mathrm{N_2}\right)\rightarrow\nu_{\mathrm{CO2}}\mathrm{CO_2}+\nu_{\mathrm{H2O}}\mathrm{H_2O}+\nu_{\mathrm{N2}}n\mathrm{N_2}+H_v \tag{11}$$

where H_v is the heat of combustion which must be specified from a knowledge of the fuel. Although five chemical species are involved such as fuel (CH_4), oxygen, carbon dioxide, water vapor and nitrogen, only three different equations for fuel, oxygen, and products (CO_2+2H_2O) are solved. CO_2 and H_2O mass fractions are obtained from the following algebraic expressions

$$Y_{\mathrm{CO_2}}=\gamma_{\mathrm{CO_2}}Y_{pr} \tag{12}$$

$$Y_{\mathrm{H_2O}}=\left(1-\gamma_{\mathrm{CO_2}}\right)Y_{pr} \tag{13}$$

where,

$$\gamma_{\mathrm{CO_2}}=\nu_{\mathrm{CO_2}}W_{\mathrm{CO_2}}/\left(\nu_{\mathrm{CO_2}}W_{\mathrm{CO_2}}+\nu_{\mathrm{H_2O}}W_{\mathrm{H_2O}}\right) \tag{14}$$

and remaining mass fraction of N_2 is obtained from the condition that the sum of mass fractions is unity :

$$Y_{\mathrm{N_2}}=1-\left(Y_{fu}+Y_{\mathrm{O_2}}+Y_{\mathrm{CO_2}}+Y_{\mathrm{H_2O}}\right) \tag{15}$$

Finally, to seek mean reaction rate $\dot{\omega}_i$ in the species equation (5) due to gaseous combustion must be determined, the eddy-break up concept of Magnussen and Hjertager [7] is followed here. In this model, the mixing-controlled rate of reaction is related to the density, turbulent time scale k/ε, and the chemical species mass fraction, and the reaction rate of fuel $\dot{\omega}_{fu}$ is taken as the smallest of the turbulent dissipation rates of fuel, oxygen and products :

$$\dot{\omega}_{fu}=-\rho\frac{\varepsilon}{k}A_{EBU}\min\left[Y_{fu}, Y_{\mathrm{O_2}}/\mathrm{s}, B_{EBU}Y_{pr}/(1+s)\right] \tag{16}$$

where s is the stoichiometric oxygen/fuel ratio, and A_{EBU} and B_{EBU} are the empirical proportionality constants, taken as 4 and 0.5, respectively, in this study.

The remaining reaction rates are related to $\dot{\omega}_{fu}$, via following expression based on a single step reaction, such as

$$\dot{\omega}_{fu}=\dot{\omega}_{\mathrm{O_2}}/s=-\dot{\omega}_{pr}/(1+s) \tag{17}$$

D. The Thermodynamic Properties

The density of mixtures of air, fuel and the combustion products can be represented by the following equation of state :

$$\rho=\frac{P}{RT\sum_j Y_j/W_j} \tag{18}$$

where R is the universal gas constant. The specific heat of mixture is obtained from

$$C_{p,mix}=\sum_j Y_j C_{pj} \tag{19}$$

where,

$$C_{pj}=a_{0j}+b_{0j}T \tag{20}$$

is the specific heat of each species j. To obtain temperature from given specific enthalpy and species mass fractions, Eq. (4) is expanded into second-order polynomial for temperature, which is then calculated by using the root formula.

E. The Radiative Heat Transfer

The source term due to radiation in enthalpy equation is the divergence of the radiative heat flux [8]

$$-\nabla\cdot q^R=\kappa_a\left(4\pi I_b-\int_{4\pi} I d\Omega\right) \tag{21}$$

The absorption coefficient is modeled following the work of Khalil *et al*. [11] as $\kappa_a=0.2Y_{fu}+0.1Y_{pr}$, while the scattering is neglected. The radiative intensity can be obtained by using the finite volume method for radiation [9,10]

III. Solution Procedure

The general form of the governing transport equations for turbulent reacting flows above mentioned can be written as the following form :

$$\frac{\partial}{\partial x_j}\left(\rho u_j\phi\right)=\frac{\partial}{\partial x_j}\left(\Gamma_\phi\frac{\partial\phi}{\partial x_j}\right)+S_\phi \tag{22}$$

where ϕ is the dependent variables representing u, v, w, h, and Y_i. Γ_ϕ and S_ϕ are the diffusion coefficients and source terms for each ϕ, respectively, as shown in Table 1. These

TABLE I
VARIABLES AND SOURCE TERMS APPEARING IN EQ. (22)

ϕ	Γ_ϕ	S_ϕ
u	μ_{eff}	$-\frac{\partial p}{\partial x}+\frac{\partial}{\partial x}\left(\mu_{eff}\frac{\partial u}{\partial x}\right)+\frac{\partial}{\partial y}\left(\mu_{eff}\frac{\partial v}{\partial x}\right)+\frac{\partial}{\partial z}\left(\mu_{eff}\frac{\partial w}{\partial x}\right)$
v	μ_{eff}	$-\frac{\partial p}{\partial y}+\frac{\partial}{\partial x}\left(\mu_{eff}\frac{\partial u}{\partial y}\right)+\frac{\partial}{\partial y}\left(\mu_{eff}\frac{\partial v}{\partial y}\right)+\frac{\partial}{\partial z}\left(\mu_{eff}\frac{\partial w}{\partial y}\right)$
w	μ_{eff}	$-\frac{\partial p}{\partial z}+\frac{\partial}{\partial x}\left(\mu_{eff}\frac{\partial u}{\partial z}\right)+\frac{\partial}{\partial y}\left(\mu_{eff}\frac{\partial v}{\partial z}\right)+\frac{\partial}{\partial z}\left(\mu_{eff}\frac{\partial w}{\partial z}\right)$
k	$\frac{\mu_{eff}}{\sigma_k}$	$G-\rho\varepsilon$
ε	$\frac{\mu_{eff}}{\sigma_\varepsilon}$	$\frac{\varepsilon}{k}\left(C_{\varepsilon 1}G-C_{\varepsilon 2}\rho\varepsilon\right)$
h	$\frac{\mu_{eff}}{\mathrm{Pr}_T}$	$H_v\dot{\omega}_{fu}-\nabla\cdot q^R$
Y_{fu}	$\frac{\mu_{eff}}{\mathrm{Sc}_T}$	$-\dot{\omega}_{fu}$
Y_{O_2}	$\frac{\mu_{eff}}{\mathrm{Sc}_T}$	$-\frac{2W_{\mathrm{O}_2}}{W_{fu}}\dot{\omega}_{fu}$
Y_{pr}	$\frac{\mu_{eff}}{\mathrm{Sc}_T}$	$\frac{\left(W_{\mathrm{CO}_2}+2W_{\mathrm{H}_2\mathrm{O}}\right)}{W_{fu}}\dot{\omega}_{fu}$

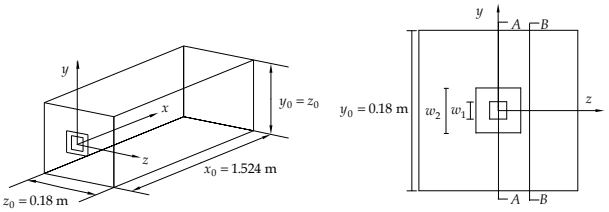

Fig. 1 Schematics of the problem : three-dimensional combustion chamber (left), inlet plane (right)

governing equations are expressed in the finite-difference form and solved by using collocated grid system following the work of Cho [12]. Cho [12] examined such various problems as three-dimensional lid-driven cavity, square and circular curved duct, circular to rectangular transition duct, and magnetic flowmeter by using the code named CMJ3D, which is employed in this study to find turbulent internal flow in combustion chamber. More detailed information are discussed in Cho [12].

The inflow nozzle, composed of separate fuel and combusting air tubes as illustrated in Fig. 1, has fixed quantities according to each working gas entered. In the walls, no slip for momentum, wall function for turbulence, adiabatic energy balance for enthalpy, and Neumann conditions for chemical species are adopted, respectively. In the exit plane, which is located fully downstream not to affect the internal flow, the mean flux is adjusted to ensure overall continuity, as usually adopted in SIMPLE method. All other quantities including k, ε, h and Y_i are treated as Neumann condition with zero gradient. Special care should be taken in the calculation of the radiative intensity. The inflow and exit planes act as black walls

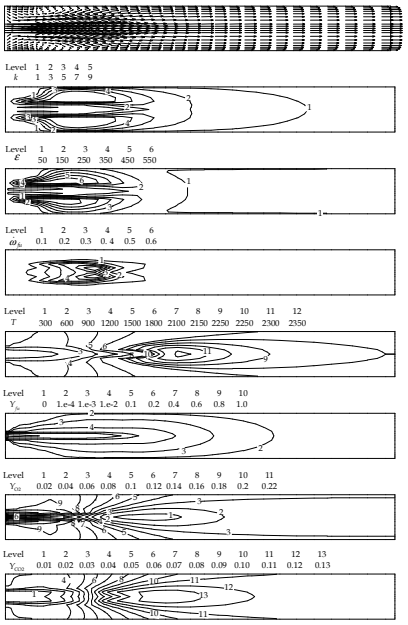

Fig. 2 Contour plots for $\lambda = 0.8$ at center plane without swirl

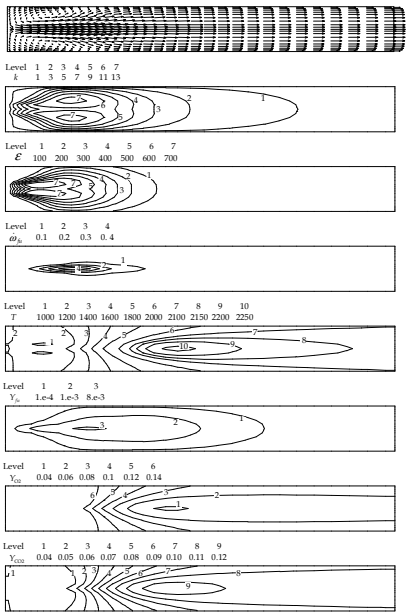

Fig. 3 Contour plots for $\lambda = 0.8$ at $z = 0.033$m without swirl

kept at T_{air}, T_{CH_4}, and 300 K for air, fuel tubes and exit plane, respectively, not to disturb internal radiation field.

IV. RESULTS AND DISCUSSION

Fig. 1 illustrates the schematic of the three-dimensional combustion chamber adopted in this work. The chamber has a $(w_1 \times w_1)$ fuel tube enveloped in the $(w_2 \times w_2)$ outer air tube, both are centered axially in a (18×18) cm^2 wide by 1.524 m long test section. The velocity of combustion air with

$T_{air} = 600\,\mathrm{K}$ is $15\,\mathrm{m/s}$, while the velocity of fuel kept at $T_{fu} = 300\,\mathrm{K}$ varies as $4.41\lambda u_{air}\ \mathrm{m/s}$ according to the eqivalence ratio, where u_{air} is the inlet air velocity. The fuel used in this case is gaseous CH_4. A grid system is $(N_x \times N_y \times N_z) = (35\times19\times19)$ and $(N_\theta \times N_\phi) = (4\times8)$ for spatial and angular domain, respectively.

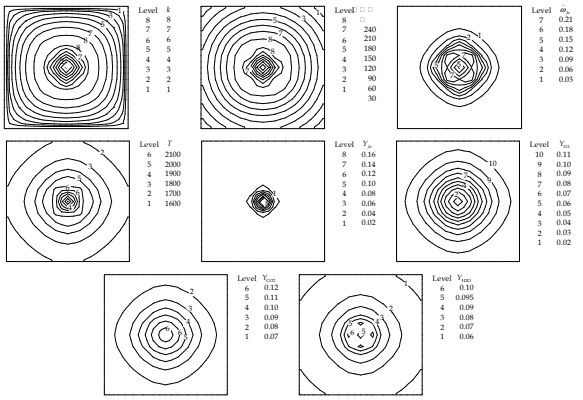

Fig. 4 Contour plots for $\lambda = 0.8$ at $x = x_0/2$ plane without swirl

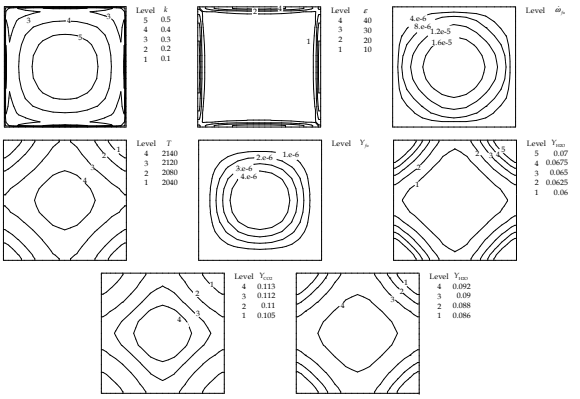

Fig. 5 Contour plots for $\lambda = 0.8$ at exit plane without swirl

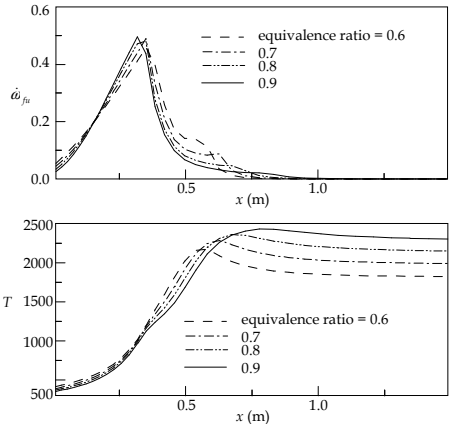

Fig. 6 Effect of equivalence ratio on reaction rate and temperature for the case of without swirl

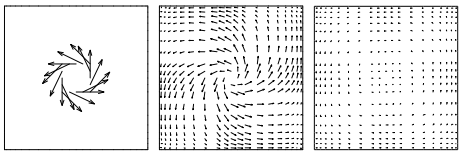

Fig. 7 The velocity vector plots on various cross sections for the case of swirling angle of 30° with $\lambda = 0.8$

Fig. 2 presents the velocity vectors and contour plots for the case of $\lambda = 0.8$ without swirl at $z = 0$ plane (A-A plane in Fig. 1). The turbulent kinetic energy and dissipation rate of turbulent kinetic energy are similar to those over a backward-facing step. It is seen that maximum reaction rate is formed in the region where turbulent quantities are more active, and high temperature is found in the central zone. The mass fraction of fuel, oxidizer, CO_2, and H_2O is also shown in Fig. 3. The mass fraction of fuel indicates that reaction is active near the inlet and most of the fuel is consumed, where mixing is intense due to abrupt expansion and resulting high turbulent quantities. The oxidizer is consumed as the reaction progresses, and has a minimum value behind where the maximum reaction rate occurs. The contour of the products mass fraction are similar to that of temperature. Fig. 3 shows the flow and combustion quantities at $z = 0.33\,\mathrm{m}$ plane (B-B plane in Fig. 1). Note that all the quantities are similar to those in center A-A plane.

Figs. 4 and 5 indicate k, ε, $\dot{\omega}_{fu}$, T, Y_{fu}, Y_{O_2}, Y_{CO_2} and Y_{H_2O} at different two axial locations of $x = x_0/2$ and $x = x_0$ planes. It is seen that while the flow is not fully developed and reaction is in progress in $x = x_0/2$ plane, the flow is developed and reaction terminated, therefore unburned oxygen and combustion products exits the combustor.

The effect of equivalence ratio is examined by varying the inlet fuel velocity u_{fu} with a fixed inlet air velocity of $u_{air} = 15\,\mathrm{m/s}$. Fig. 6 depicts the variation of the reaction rate of fuel, temperature and CO_2 mass fraction at the centerline. As the equivalence ratio changes from 0.6 to 0.9, temperature and CO_2 mass fraction increases slowly but reaches higher value at the exit, although reaction is not changed significantly.

In most of the industrial combustor such as gas turbine and pulverized coal combustor, there often exists swirling air to hence the mixing between the fuel and combustion air and stabilize the flame. Fig. 7 shows velocity vectors at various axial locations when the swirling angle of combustion air at the inlet tube is 30° with respect to the axial axis. As expected, the tangential velocity vanishes as the flow moves downstream. Because of swirling air, more intense mixing is found as shown in Fig. 8 compared with the case of no swirl in Figs. 2 and 3. Also, reaction occurs near the inlet and the flame moves upstream. It is also seen that most of the fuel is consumed upstream due to the swirling velocity, and the products are formed near the inlet. More intense mixing is also found in z=0.033m (B-B) plane as shown in Fig. 9. Unlike the center

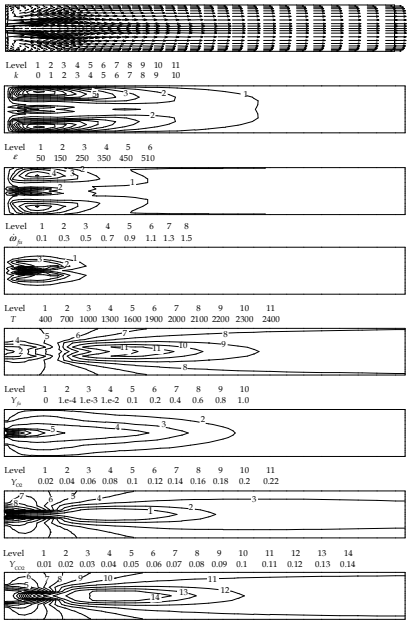

Fig. 8 Contour plots for $\lambda = 0.8$ at center (z=0) plane with swirl angle of 30 degree

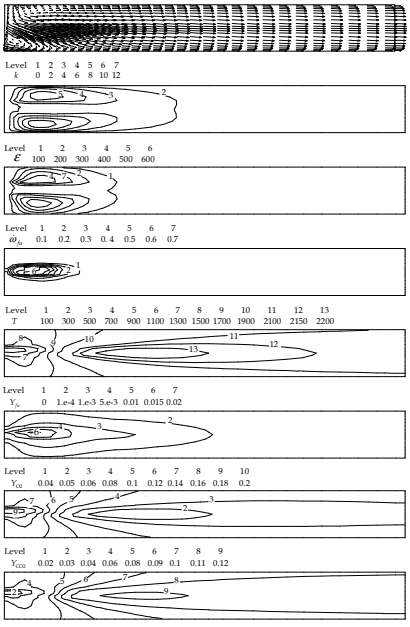

Fig. 9 Contour plots for $\lambda = 0.8$ at z=0.033m plane with swirl angle of 30 degree

A-A plane, however, distortion in contours is observed due to swirling air. Figs. 10 and 11 show the flow and combustion variables obtained at both $x = x_0/2$ and $x = x_0$ planes.

The reaction rate of fuel, temperature and CO_2 mass fraction at the centerline are compared at various swirling angles in Fig. 12. As the swirling angle increases from 0 to 45°, i.e., tangential velocity of combustion air increases from 0 to 15m/s, the reaction rate of fuel moves upstream, as is temperature and

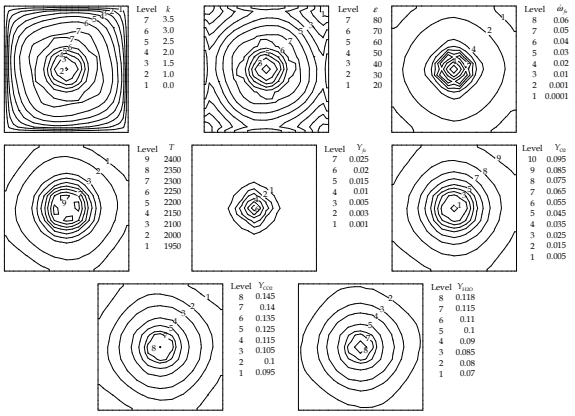

Fig. 10 Contour plots for $\lambda = 0.8$ at $x = x_0/2$ plane with swirl angle of 30 degree

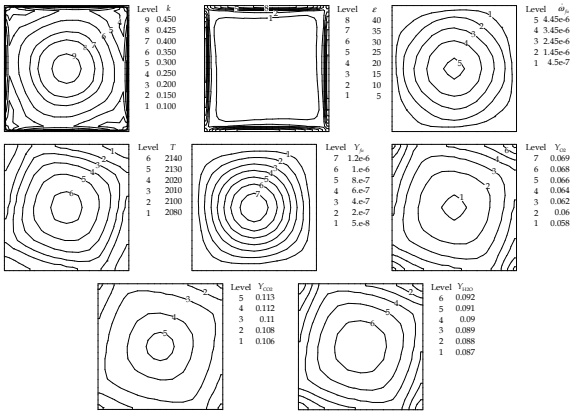

Fig. 11 Contour plots for $\lambda = 0.8$ at exit ($x = x_0$) plane with swirl angle of 30 degree

CO_2 mass fraction. Fig. 13 shows variation of reaction rate of fuel, temperature and CO_2 mass fraction at the centerline, in both cases of with and without radiation. However, it is found that there is only small difference between two cases regardless of the equvalence ratio. Therefore, it is concluded that thermal radiation does not plat a significent role in this combustion chamber.

V. Conclusion

In this work, numerical analysis has been carried out to investigate the combustion characteristics in a three-dimensional combustion chamber. The applied mathematical models for prediction of velocities, turbulence quantities, enthalpy and chemical species concentration involved have been described and discussed in detail. Turbulent combustion has been modeled by using the eddy-break up model, while in modeling the radiative heat transfer finite-volume method for radiation has been used. As the equivalence ratio increases, which means that more fuel is supplied due to a larger inlet fuel velocity, the flame temperature increases and the location of maximum temperature has moved towards downstream. In the mean

while, the existence of inlet swirling air velocity makes the fuel and combustion air more completely mixed and burnt in short distance. Therefore, the locations of the maximum reaction rate and temperature were shifted to forward direction compared with the case of no swirl. It is also found that thermal radiation has only a minor effect on combustion characteristics in this type of combustor, although it slightly lower the flame temperature.

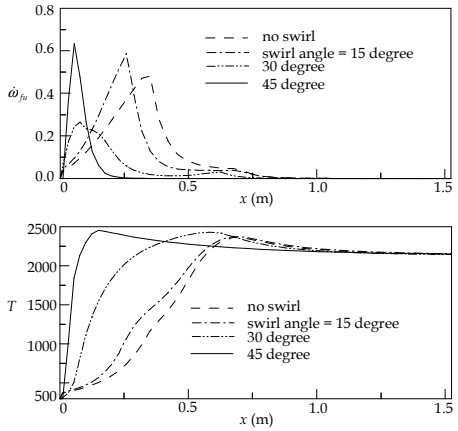

Fig. 12 Effect of swirl angle on reaction rate and T

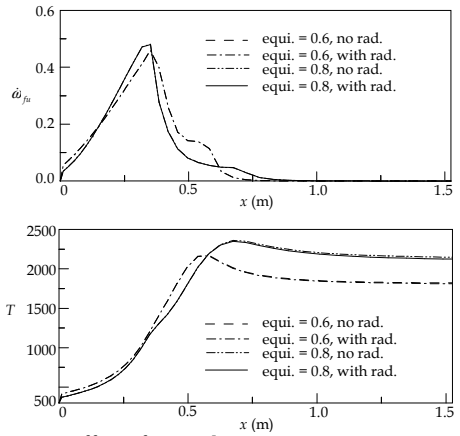

Fig. 13 Effect of equivalence ratio on reaction rate and T

It is expected that the approaches adopted in this work can be applied to the investigation of turbulent combustion in practical combustors with the formation of combustion-generated pollutants such as NO and CO.

ACKNOWLEDGMENT

This research was supported by Basic Science Research Program through the National Research Foundation of Korea (NRF) funded by the Ministry of Education, Science and Technology (grant number 2011-0022179). Also, this work was partially supported by Leading Foreign Research Institute Recruitment Program through the National Research Foundation of Korea funded by the Ministry of Education, Science and Technology (2011-0030065).

REFERENCES

[1] S. M. Correa, and W. Shyy, "Computational Models and Methods for Gaseous Turbulent Combustion," *Progress in Energy and Combustion Science*, vol. 13, pp. 249-292, 1987.
[2] A. K. Gupta, and D. G. Lilley, "Combustion and Environmental Challenges for Gas Turbines in the 1990s," *Journal of Propulsion and Power*, vol. 10, no. 2, pp. 137-147, 1994.
[3] M. C. Drake, and R. J. Blint, "Relative Importance of Nitric Oxide Formation Mechanism in Laminar Opposed-Flow Diffusion Flames," *Combustion and Flame*, vol. 83, nos. 1/2, pp. 185-203, 1991.
[4] J.-Y. Chen, and W. Kollamn, W., "PDF Modeling and Analysis of Thermal NO Formation in Turbulent Nonpremixed Hydrogen-Air Jet Flames," *Combustion and Flame*, vol. 88, nos. 3/4, pp. 397-412, 1992.
[5] J. A. Miller, and C. T. Bowman, "Mechanism and Modeling of Nitrogen Chemistry in Combustion," *Progress in Energy and Combustion Science*, vol. 15, pp. 287-338, 1989.
[6] B. E. Launder, and D. B. Spalding, "The Numerical Computation of Turbulent Flows," *Computer Methods in Applied Mechanics and Engineering*, vol. 3, pp. 269-289, 1974.
[7] B. F. Magnussen, and B. H. Hjertager, "On Mathematical Modeling of Turbulent Combustion with Emphasis on Soot Formation and Combustion," *16th Symposium (International) on Combustion*, The Combustion Institute, Pittsburgh, PA, pp. 719-729, 1976.
[8] S. W. Baek, M. Y. Kim, and J. S. Kim, "Nonorthogonal Finite-Volume Solutions of Radiative Heat Transfer in a Three-Dimensional Enclosure," *Numerical Heat Transfer, Part B (Fundamentals)*, vol. 34, no. 4, pp. 419-437, 1998.
[9] M. Y. Kim, "A Heat Transfer Model for the Analysis of Transient Heating of the Slab in a Direct-Fired Walking Beam Type Reheating Furnace," *International Journal of Heat and Mass Transfer*, vol. 50, no.19-20, pp. 3740-3748, 2007.
[10] J. H. Jang, D. E. Lee, M. Y. Kim, and H. G. Kim, "Investigation of the Slab Heating Characteristics in a Reheating Furnace with the Formation and Growth of Scale on the Slab Surface," *International Journal of Heat and Mass Transfer*, vol. 53, no.19-20, pp.4326-4332, 2010.
[11] E. E. Khalil, D. B. Spalding, and J. H. Whitelaw, "The Calculation of Local Flow Parameters in Two-Dimensional Furnaces," *International Journal of Heat and Mass Transfer*, vol. 18, pp. 775-791, 1975.
[12] M. J. Cho, "An Investigation of Treatment Methods for Non-Orthogonal Terms and Wall Function Method in the Numerical Analysis of 3-D Flow Fields with Arbitrary Boundaries," Ph. D. Thesis, Korea Advanced Insititute of Science and Technology, Taejon, Korea, 1996.